ISSN 0140 3818
SSSU 31

AERODYNAMIC INTERACTION BETWEEN AN AEROFOIL AND A FREEBOARD SUPERSTRUCTURE

by C.J. Satchwell

Ship Science Report No. 31

April 1987

AERODYNAMIC INTERACTION BETWEEN AN AEROFOIL AND A FREEBOARD/SUPERSTRUCTURE

By

C.J. Satchwell

ABSTRACT

A description is given of an investigation into the airloads generated (1) by an isolated freeboard/superstructure (2) by isolated aerofoils and (3) by a combination of freeboard/superstructure and aerofoils. A formula is derived to describe the airloads on an isolated freeboard/superstructure, which compares favourably with test data. This is of interest for calculating ship air resistance. Airloads due to the interaction airflow between an aerofoil and superstructure are found to be propulsive. The variation of interaction airloads with varying freeboard and aerofoil/deck gap are described.

NOMENCLATURE

α	–	incidence of marine aerofoil
α_i	–	induced angle of attack
β	–	incidence of hull
A	–	aspect ratio of hull = 2 x freeboard/length o.a.
C_{LH}	–	hull lift coefficient = hull lift/($\frac{1}{2}\rho U^2$ x freeboard x length o.a.)
C_{LD}	–	hull drag coefficient = hull drag/($\frac{1}{2}\rho U^2$ x freeboard x length o.a.)
C_{LA}	–	aerofoil lift coefficient = aerofoil lift/($\frac{1}{2}\rho U^2$ x aerofoil area)
C_{DA}	–	aerofoil drag coefficient = aerofoil drag/($\frac{1}{2}\rho U^2$ x aerofoil area)
k	–	independent constants, used in induced drag formulae for high and low aspect ratio wings (see Section V)
ΔC_L	–	interaction lift coefficient } Defined in Section III
ΔC_D	–	interaction drag coefficient
C_{DO}	–	profile drag coefficient

I. INTRODUCTION

Vortex shedding from a ship freeboard/superstructure can produce an interaction with trailing vortices from a marine aerofoil, to beneficially affect the airload from that aerofoil. This effect is noted in ref (1), where the combination of a sail and hull is shown to produce more drive than that of a sail alone, despite the fact that air resistance is normally associated with a hull. More general work on ship air resistance (e.g. refs (2) and (3)) is usually concerned with quantifying total air resistance and its effect on ship performance, rather than providing an insight into the nature of the flow.

The present investigation involves force measurements of a hull alone, aerofoil alone and hull/aerofoil combination. Configuration was that of a typical wind-assisted ship. Insight into the nature of the flow was obtained indirectly, by comparing trends in aerodynamic forces with other shapes whose surrounding flows are well known.

Primary motivation for the work comes from a need to predict the propulsive benefits of a marine aerofoil fitted to an arbitrary freeboard/superstructure, as well as a requirement to fit a marine aerofoil in a location where it can do most good. These broad issues have not been resolved by this single set of experiments, although the information presented on interaction airloads for typical wind-assisted ship configurations should be useful for many performance estimates.

II APPARATUS AND TECHNIQUE

Design of a suitable model to investigate hull/aerofoil vortex interaction effects involved requirements to:

a) Simulate the flow around a ship freeboard/superstructure as closely as possible, preventing self-cancellation of adjacent vortices and maintaining a pressure seal at the waterline. Ideally, windspeed/height and wind direction/height effects should also be included.

b) Measure the forces on the hull alone, aerofoil alone or hull/aerofoil combination.

c) Allow a wide variety of configurations to be tested, with rapid configuration changes.

The flow simulation requirements could probably have been met by a conventional ship freeboard/superstructure model, without a pressure seal at the waterline. This option would have resulted in additional vortices shed from the waterline region. For this initial investigation, it was felt that such unrepresentative vortex shedding in the proximity of other hull vortices should be avoided, although it is acknowledged that there may be a case for having waterline vortices to simulate velocity gradient effects. Accordingly, it was decided to use an image model, with a splitter plate in the vicinity of the hull vortices, to ensure that separate vortex identities were maintained. Wind velocity gradient effects were left for future investigations.

The rig was designed to be attached to a conventional three-component wind tunnel balance. A diagram of the rig is shown in Fig 1. Principal components are the segemented aerofoils, the segmented image freeboard/superstructure model and a rod to simulate a mast.

Tests were carried out for the following aerofoil/hull combinations:

Aerofoil: 7/8 span (used for all tests involving aerofoils)

Draft:	Load	Medium	Ballast
Gap:	Nil	1/8 span	1/4 span

Tests were carried out for the following hull configurations, without aerofoils present:

Draft:	Load	Medium	Ballast

Tests were carried out with aerofoils alone, using spacings corresponding to the width of the hull model at medium draft with Nil, 1/4 span, and 1/2 span additional gaps.

In addition, tare tests were carried out to establish the drag of the struts and mast. The mast was present during all tests involving aerofoils and/or hulls.

Variable span can be simulated by varying the number of aerofoil segments, a variable hull/aerofoil gap by moving the segments along the rod and a variable freeboard by varying the number of segments in the ship superstructure model. Variable apparent wind angle (β) is achieved by varying the angle of the hull model relative to the flow using an adjustable rear support wire and varaible incidence (α) by varying the angle of the mast relative to the centreline of the hull. Angles were measured to $.1^{\circ}$ by a digital clinometer.

The freeboard/superstructure image model was based on the large oil tanker 'Bulford', whose details are given in ref (8). Those details are for the load draft (i.e. with no removable segments). Configurations tested were for load, medium and ballast draft conditions. Medium and ballast draft tests on the model of the large vessel may be representative of flow conditions around a smaller vessel at load draft, although some allowance for superstructure scaling may be needed.

A test programme was designed around limited wind tunnel time in a 5' x 7' low-speed tunnel at Southampton University. It was clear that all combinations of all variables would represent too large a programme for the available time, and so a datum condition was selected and an investigation made into the effects of changing single parameters. It was also felt that the stalled operation of the aerofoil was not of interest within the range $0^{\circ} < \beta < 45^{\circ}$ and so tests of a particular configuration were stopped whenever a stall had clearly been passed.

Flexibility in the balance struts produced vibrational problems at high tunnel speeds and the final speed chosen (24.38 m/s) was the highest speed at which vibrational problems were consistently absent. This speed was used for all tests. The corresponding Reynolds Number (based on aerofoil chord) was around 250,000.

III RESULTS AND DATA ANALYSIS

Results were obtained in the form of lift and drag measurements from the wind tunnel balance. Speeds were corrected for blockage according to the formula given in ref (5) for arbitrary forms, i.e.

$$\varepsilon_t = \frac{1}{4} \cdot \frac{\text{model frontal area}}{\text{test section area}}$$

Tare tests established the contributions of the struts and exposed sections of rod to the total measured forces and these were deducted to obtain forces for the test configurations.

Aerodynamic coefficients for the hull are non-dimensionalised on the longitudinal profile freeboard area (i.e. the area of freeboard seen when a ship is viewed from athwartships). These are plotted as a function of apparent wind angle (β) on Figs 2-7 for the three draft conditions tested.

Lift and drag coefficients for the aerofoil tests were plotted and found to follow the expected trend of $C_D = C_{DO} + kC_L^2/\pi AR$. A least-squares fit of the data for the three spacings tested (corresponding to a distance of medium draft with zero, 1/8 span and 1/4 span gaps) yielded the following results for C_{Do} and $k/\pi AR$:

Table 1

Values of Drag Constants for Tests on Isolated Aerofoils

	C_{Do}	$k/\pi AR$
Med Draft, zero gap	.0296	.1867
Med Draft, 1/8 span gap	.0315	.2009
Med Draft, 1/4 span gap	.0317	.2035

Aerofoil/hull combinations were tested at a range of apparent wind angles (β). For each value of β, a range of aerofoil incidences (α) were tested. Values of α were chosen to be representative of probable aerofoil operation.

Results for aerofoil/hull combinations are related to expectations from the results of tests on isolated aerofoils and hulls. The beneficial vortex interaction referred to in the introduction should produce an improvement to the apparent aerofoil lift and drag. This improvement can be non-dimensionalised on the aerofoil area and expressed as increments:

$$\Delta C_L = [\text{Lift}_{(\text{HULL+AEROFOILS})} - \text{Lift}_{(\text{HULL})} - \text{Lift}_{(\text{AEROFOILS})}]/\tfrac{1}{2}\rho U^2 S$$

$$\Delta C_D = [\text{Drag}_{(\text{HULL+AEROFOILS})} - \text{Drag}_{(\text{HULL})} - \text{Drag}_{(\text{AEROFOILS})}]/\tfrac{1}{2}\rho U^2 S$$

This representation is appropriate to the problem of determining the overall performance of some marine aerofoil/hull combination, although it should be appreciated that some of the force increment comes from changes to lift and drag on the hull. The usual problem posed to windship researchers involves the net propulsive force obtained when an aerofoil is close to a hull, and not how that net propulsive force is subdivided into aerofoil and hull components. For this performance problem, hull interaction effects can be accounted for by adding ΔC_L and ΔC_D on to estimated coefficients for isolated aerofoils.

Results involve the differences of very similar quantities and considerable scatter. Preliminary plots of C_D v. C_L based on $\text{Force}_{(\text{HULL+AEROFOILS})} - \text{Force}_{(\text{HULL})}$ showed no obvious trend to converge or diverge from similar plots for isolated aerofoils, although it has to be said that any such trend could have been masked by scatter. For a given β, draft and gap, the effect of the airflow interaction appeared similar to a change in C_{Do} and essentially independent of C_L. Accordingly, priority was then given to reducing scatter, by averaging ΔC_L and ΔC_D for all the representative

unstalled incidences in a particular configuration. Results are shown in Figs 8 and 9 as graphs of ΔC_L and ΔC_D plotted against β.

IV INTERPRETATION OF RESULTS

(1) Isolated Hull Results:

Data for the isolated hull tests are of interest for weather routeing research and easily-programmable formulae were sought to represent the data. Previous work in this area, e.g. ref (2) involved the use of general regression formulae and made no claims to relate to the underlying physics of the flow. Any simple formula is unlikely to be effective unless related to the flow processes involved and so a conceptual flow model was sought from which a suitable formula could be deduced.

In ref (6) square aircraft fuselages and similar shapes are treated as low-aspect-ratio wings. In ref (7) low-aspect-ratio wing theory is not specifically mentioned, although a formula is quoted whose origins may lie in the theory. A summary of low-aspect-ratio wing theory is given in ref (6). Deductions from this summary show that C_L and C_D take the form:

$$C_L = k \sin^2\alpha\cos\alpha + a.\alpha \qquad (1)$$

$$C_D = C_{Do} + a.\alpha.\tan\alpha i + k \sin^3\alpha \qquad (2)$$

In equation (1) terms involving a constant 'k' represent the lift produced by a vortex, generated near the front of a wing, inducing low pressures on the upper surface; whereas terms involving the constant 'a' relate to normal lift from bound vorticity. The valid incidence range of these expressions is also questionable, since when $\alpha = \pi/2$ no lift could be expected from a fully-stalled wing. Some modification to low-aspect-ratio wing formulae is needed to ensure that they converge to the right answers for both high and low incidences.

Firstly, with very low aspect ratio wings it will be assumed that secondary lift (from leading edge vortices) is very much greater than

lift from bound vorticity. Secondly, it will be assumed that the efficiency of the secondary-lift-producing process will become less than indicated by conventional formulae by some factor $f(\beta)$. Thirdly, it is convenient to separate parasite (C_{Do}) components of the drag coefficient so as to enable vortical and separation effects to be treated separately. Now for a hull inclined at an incidence 'β' relative to the airflow, these ideas produce formulae for hull lift and drag coefficients which take the form:

$$C_L = f(\beta) \cdot k \sin^2\beta\cos\beta \qquad (3)$$

$$C_{Di} = f(\beta) \cdot k \sin^3\beta \qquad (4)$$

Now $f(\beta)$ needs to be 1 when $\beta = 0$, 0 when $\beta = \pi/2$ and approximately 1 throughout the normal range of applciability of low-aspect-ratio wing formulae i.e. $0<\beta<.4$. Various least-squares regressions of test data with different forms of $f(\beta)$ were tried and a good fit obtained with $f(\beta) = \cos\beta$. If 'k' is arbitrary, then any corrections for constants can be introduced via 'k' and (3) and (4) may be written:

$$C_L = k \cdot \sin^2 2\beta \qquad (5)$$

$$C_{Di} = k \cdot \tan\beta \sin^2 2\beta \qquad (6)$$

Values of k were found (via least squares regression) for the three isolated hull configurations and found to be reasonably linear with hull aspect ratio.

A final version of the formulae which included aspect ratio (A) effects was found by further regression to be:

$$C_{LH} = (.2554 + 1.933A) \sin^2 2\beta \qquad (7)$$

$$C_{DiH} = (.2554 + 1.933A) \cdot \tan\beta \sin^2 2\beta \qquad (8)$$

Equation 7 is plotted as a continuous line on Figs (2), (3) and (4).

Agreement is reasonably good. Equation 8 provided a guide for induced drag components of measured drag coefficients and this enabled parasite drag coefficients to be estimated as:

$$C_{DOH} = C_{DH} - C_{LH} \tan\beta \tag{9}$$

Physical arguments for the parasite drag coefficients are harder to find. It was envisaged that there might be two components of parasite drag, one dependent on a frontal profile (C_{DOF}) and another dependent on a lateral profile (C_{DOL}). It can be argued that drag coefficients will themselves depend on some function of β, as does the area presented by these profiles to the airflow. These arguments led to a trial function for C_{DOH} as:

$$C_{DOH} = \cos^2\beta \cdot C_{DOF} + \sin^2\beta \cdot C_{DOL} \tag{10}$$

A least-squares regression of drag test data gave an expression for C_{DOH} as:

$$C_{DOH} = \frac{.03205}{A^{.6743}} \cdot \cos^2\beta + \frac{.009477}{A^{1/3183}} \sin^2\beta \tag{11}$$

The final expression for C_{DH} is therefore:

$$C_{DH} = \frac{.03205}{A^{.6743}} \cdot \cos^2\beta + \frac{.009477}{A^{1.3183}} \sin^2\beta + (.2554 + 1.933A) \tan\beta \cdot \sin^2 2\beta \tag{12}$$

Equation (12) is plotted on Figs (5), (6) and (7), where it can be compared with the measured data. Agreement is good, which suggests that there are similarities between the flow around a ship freeboard/superstructure and that around a low-aspect-ratio wing; since low aspect ratio wing formulae form the basis of expressions for C_{LH} and C_{DH}.

As beam/length ratio increases, then the frontal area increases and the contribution of the first term in equation (12) should also increase. Tests were conducted at a beam/length o.a. ratio of .1488. For ships of similar beams/length ratios, equation (12) might be tentatively scaled to reflect frontal area changes:

$$C_{DH} = \frac{.2033}{A^{.6743}} \cdot \frac{\text{beam}}{\text{length o.a.}} \cdot \cos^2\beta + \frac{.009477}{A^{1.3183}} \sin^2\beta$$

$$+ (.2554 + 1.933\ A) \tan\beta \cdot \sin^2\beta \qquad (13)$$

For air resistance calculations, it is normal to work in terms of body rather than wind axes and on this basis the resistive (x) and lateral (y) airloads are:

$$\begin{aligned} X &= (C_{DH} \cos\beta - C_{LH} \sin\beta)\ \tfrac{1}{2}\ \rho\ U^2 \times \text{freeboard} \times \text{length o.a.} \\ Y &= (C_{DH} \cdot \sin\beta + C_{LH} \cos\beta)\ \tfrac{1}{2}\ \rho\ U^2 \times \text{freeboard} \times \text{length o.a.} \end{aligned} \qquad (14)$$

where C_{LH} and C_{DH} are given by equations (7) and (13).

(ii) Hull/Aerofoil Results

Hull/aerofoil interaction effects shown in Figs (8) and (9) contain some experimental errors but nevertheless display interesting trends. Firstly, one theory that is often advanced is that where there is no gap between a hull and an aerofoil, there should be a carry-over of lift from the aerofoil to the hull in a similar manner to the carry over of lift between an aircraft wing and fuselage. If any such carry-over exists, then there should be a drag reduction at all values of β. At $\beta=0$, where the aircraft analogy is strongest, there is no clear increase in lift or reduction in drag, which suggests that there is no carry-over of lift between the hull and the aerofoil. It may be possible to redesign the upper portions of a ship to arrange for lift to be carried over to a superstructure; but in the normal context of fitting aerofoils to ships with conventional superstructures, the idea of closing the aerofoil/hull gap to remove the lower aerofoil tip vortex seems to be without value.

Figs (8) and (9) show interaction lift increases and interaction drag reductions are usually present as β is increased from zero. The analysis of hull data suggests that hull vortices are also present when $\beta>0$ and that these vortices will induce a beneficial sidewash on the aerofoil to increase lift and reduce induced drag. The Biot Sauvart Law suggests that the benefits of vortex interaction effects depend on the strengths and relative positions of the hull and aerofoil vortex systems. Unfortunately, the positions of the hull vortices are not known with any certainty, although it is reasonable to speculate that one vortex will be shed from the windward end of the bulwark and another from the leeward end, which may then stay close to the leeward freeboard. Uncertainty over the physical model makes it difficult to attempt to condense the results into simple formulae of the type used for the isolated hull data.

It is possible to identify parameters that are likely to influence the strengths and positions of hull and aerofoil vortex systems and in turn to expect these to influence lift and drag changes

attributable to interaction effects. Relevant parameters include:

Hull aspect ratio
Bulwark details
Superstructure details
Aerofoil/hull gap
Aerofoil aspect ratio
Aerofoil longitudinal position on the ship

Figs (8) and (9) show curves of ΔC_L and ΔC_D for a variety of ship loading conditions (aspect ratio) and hull/aerofoil gaps. Effects of hull aspect ratio on interaction lift (ΔC_L) are highest with the ballast draft and lowest with medium draft. For $\beta<30^o$ the effects of hull aspect ratio on interaction thrust (ΔC_D) increase with decrease in aspect ratio, however the benefits of the low aspect ratio hull in generating interaction thrust are progressively lost as β increases beyond 30^o. This may be due to a hull vortex detaching from the leeward freeboard.

Hull/aerofoil gap effects on interaction lift and thrust can be seen on Fig (8). The zero-gap case exhibits a very different trend to the other two cases of 1/8 span gap and 1/4 span gap. The zero-gap curve shows a peak in interaction lift at $\beta=15^o$ and an interaction thrust corresponding to $C_D = -.23$ at $\beta=30^o$. Although the zero-gap cannot be justified on arguments of lift carry over, it might be justified on grounds of generating useful interaction thrusts when β corresponds to a typical windward sailing condition. Models with other gaps, tested at $\beta=30^o$ show less than half the interaction thrust of the zero-gap configuration. When $\beta=45^o$, interaction lifts and thrusts were broadly similar for all configurations tested. Interaction lifts for configurations with 1/4 and 1/8 span gap show similar trends, with more interaction lift coming from the 1/8 span gap configuration. Interaction thrusts for these two configurations were also similar in trend, and once again the 1/8 span gap model produced slightly more thrust. Results for the 1/8 and 1/4 span gap configurations are consistent with expectations from the Biot Sauvart

law, where induced sidewash velocities on the aerofoil from the hull vortices should increase with decrease in gap.

V CONCLUSIONS

The preliminary investigation into hull/aerofoil vortex interaction effects has provided an indication of the nature of the airflow around an isolated freeboard/superstructure as well as the magnitude of interaction airloads.

Low aspect ratio wing theory has been successfully employed to describe the aerodynamic forces on an isolated freeboard/superstructure for low values of apparent wind angle (β). At higher values of β, a factor $f(\beta)$ needs to be applied to raw, low-aspect-ratio wing theory results to correct for effects such as vortex bursting, vortex divergence from the model and separation. For present results $f(\beta) \simeq \cos\beta$. Agreement between theory and data was better than expected. This suggests that similarities exist between the flow around a low-aspect-ratio wing and the flow around a ship freeboard/superstructure.

Interaction airloads are expressed as ΔC_L and ΔC_D values, based on the aerofoil area. Investigations into a variable aerofoil/superstructure gap show:

(1) Interaction airloads are generally beneficial, producing equivalent aerofoil drag coefficient reductions (ΔC_D) of the order of .1.

(2) Zero aerofoil/superstructure gap does not appear to produce any carry-over of lift between the aerofoil and superstructure. Zero gap does produce beneficial interaction effects in windward sailing conditions, but larger gaps tend to be better for reaching conditions.

(3) Interaction airloads from the 1/8 and 1/4 span gap configurations were broadly similar, with the 1/8 span gap showing a small performance advantage.

Effects of variable freeboard (draft) were strange. In windward conditions, interaction drag reductions were greatest with the load draft configuration, followed by medium draft and lastly ballast draft. In reaching conditions ($\beta = 45^{o}$) interaction drag reductions from variable freeboard produced an order of merit, of medium, ballast and load drafts. Interaction lifts were largest with the ballast draft, followed by the load draft and lastly the medium draft.

A number of parameters are identified in the report which are believed to influence the magnitude and position of aerofoil and hull vortices. Further experiments involving variation of these parameters should provide further insight into the nature of the interaction flow and perhaps sufficient data to develop a formula for interaction airloads.

Some speculative conclusions about the nature of the interaction airflow and airloads can be inferred from current data. Firstly, the apparent independence of ΔC_L and ΔC_D, with change in aerofoil lift, suggests that the major contribution to interaction airloads comes from the aerofoil acting as a winglet and extracting energy from the hull vortex system. A plausible hypothesis is that hull vortices tend to induce an effective increase in β in the lower regions of the aerofoil and so twist the lift vector to produce thrust. If this hypothesis is correct, then the magnitude of ΔC_L and ΔC_D should depend mostly on the aerofoil area in the vicinity of the hull, rather than overall aerofoil planform details. This hypothesis is also consistent with better-than-expected performance reports of some low-aspect-ratio Japanese commercial ship rigs.

Secondly, the curious variation of ΔC_L and ΔC_D with change in β, could be consistent with the 'winglet' explanation as hull vorticies grow stronger with increase in β, but may also diverge from the aerofoil at large values of β. The explanation might be that an aerofoil is subject to velocities induced by both windward and leeward hull vortices which initially grow in magnitude, due to

increasing hull vortex strengths, but then begin to decline at some critical angle of β, beyond which the windward hull vortex passes to leeward of the aerofoil.

These initial tests have not produced definitive explanations for all interaction airflow effects, but they have demonstrated that interaction airloads are generally beneficial and offer significant opportunities to improve the effectiveness of an aerofoil installation on a ship.

REFERENCES

(1) Marchaj, C.A. and Tanner, T. "Wind Tunnel Tests on a 1.4 Scale Dragon Rig". SUYR Report No. 14, 1963.

(2) Isherwood, R.M. "Wind Resistance of Ships". Trans. R.I.N.A., pp 327-338, 1972.

(3) Van Berlekom, W.B. "Wind Forces on Modern Ship Forms - Effects on Performance". Trans. N.E. Coast Inst. Shipbuilders and Engineers, pp 123-134, 1981.

(4) Rae, W.H. and Pope, A. "Low Speed Wind Tunnel Testing". Second Edition, John Wiley & Sons, pp 371, 1984.

(5) Hoerner, S.F. "Fluid Dynamic Drag". Hoerner Fluid Dynamics, pp (7-16) - (7-19, 1965.

(6) Norrbin, N.H. Discussion following ref (2).

(7) Munro-Smith, R. "Merchant Ship Types". I.M.E., pp 108-110, 1975.

ACKNOWLEDGEMENTS

(1) The assistance of Miss. M.T. Reddy, and other colleagues in the Department of Ship Science, University of Southampton is gratefully acknowledged.

(2) The work was carried out as part of an SERC-funded project to advance windship technology. Their support is gratefully acknowledged.

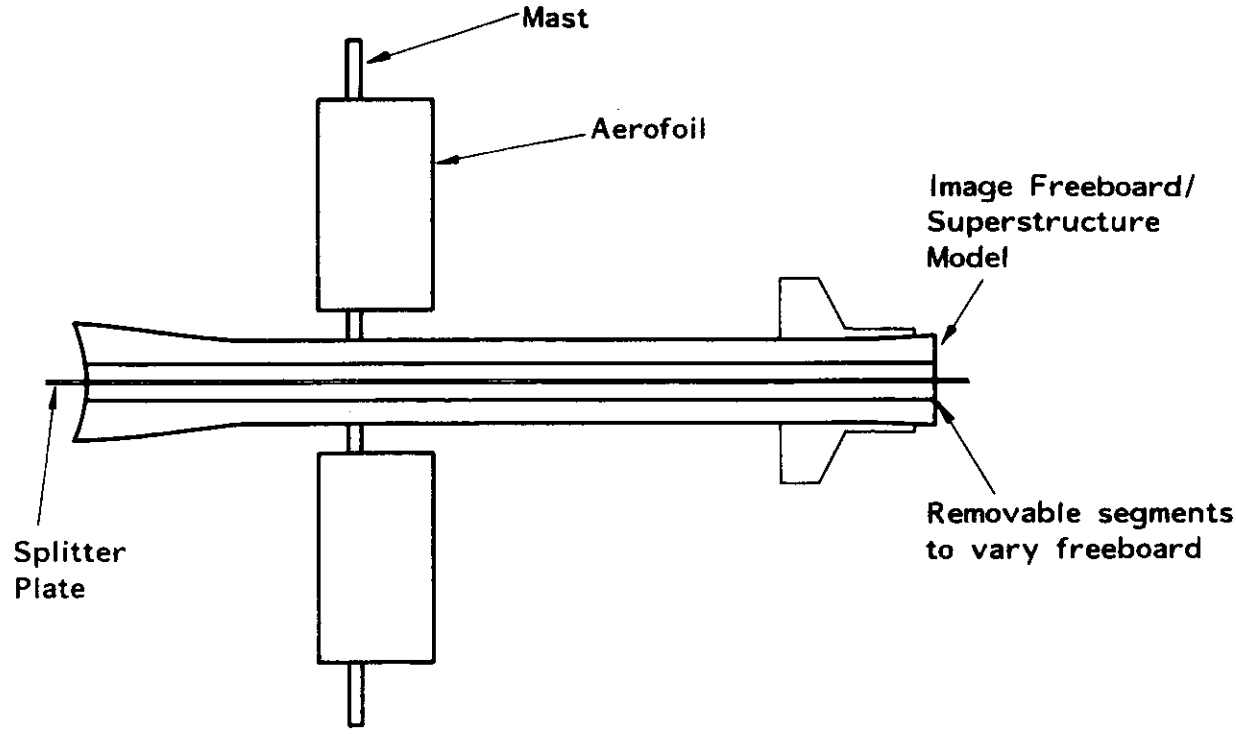

PLAN

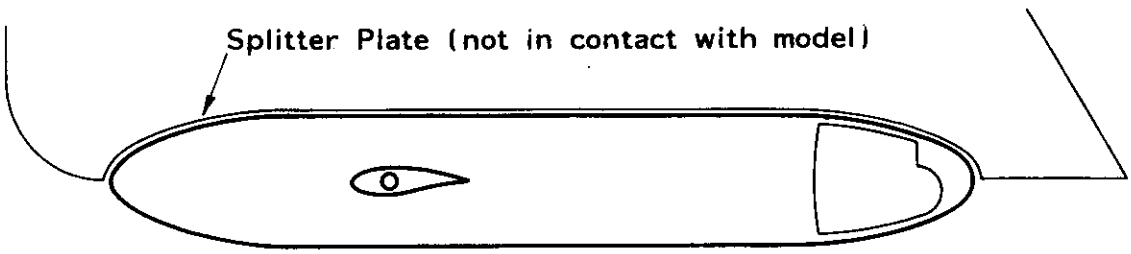

SIDE ELEVATION

$\frac{1}{10}$th scale

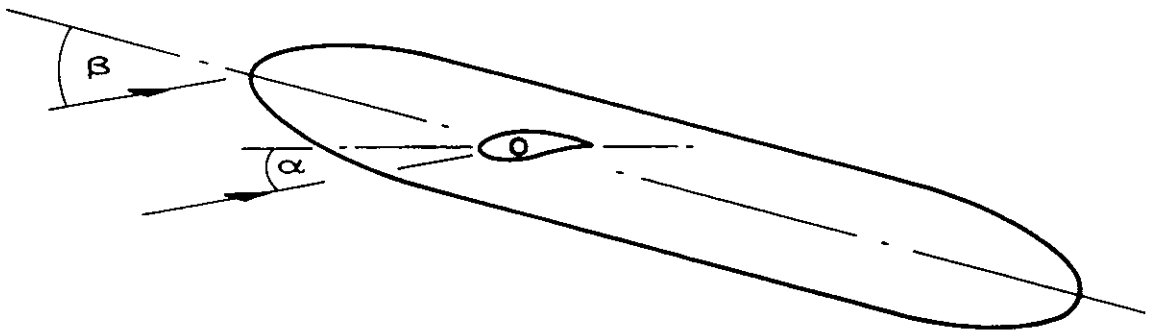

FIG. 1 MODEL DETAILS

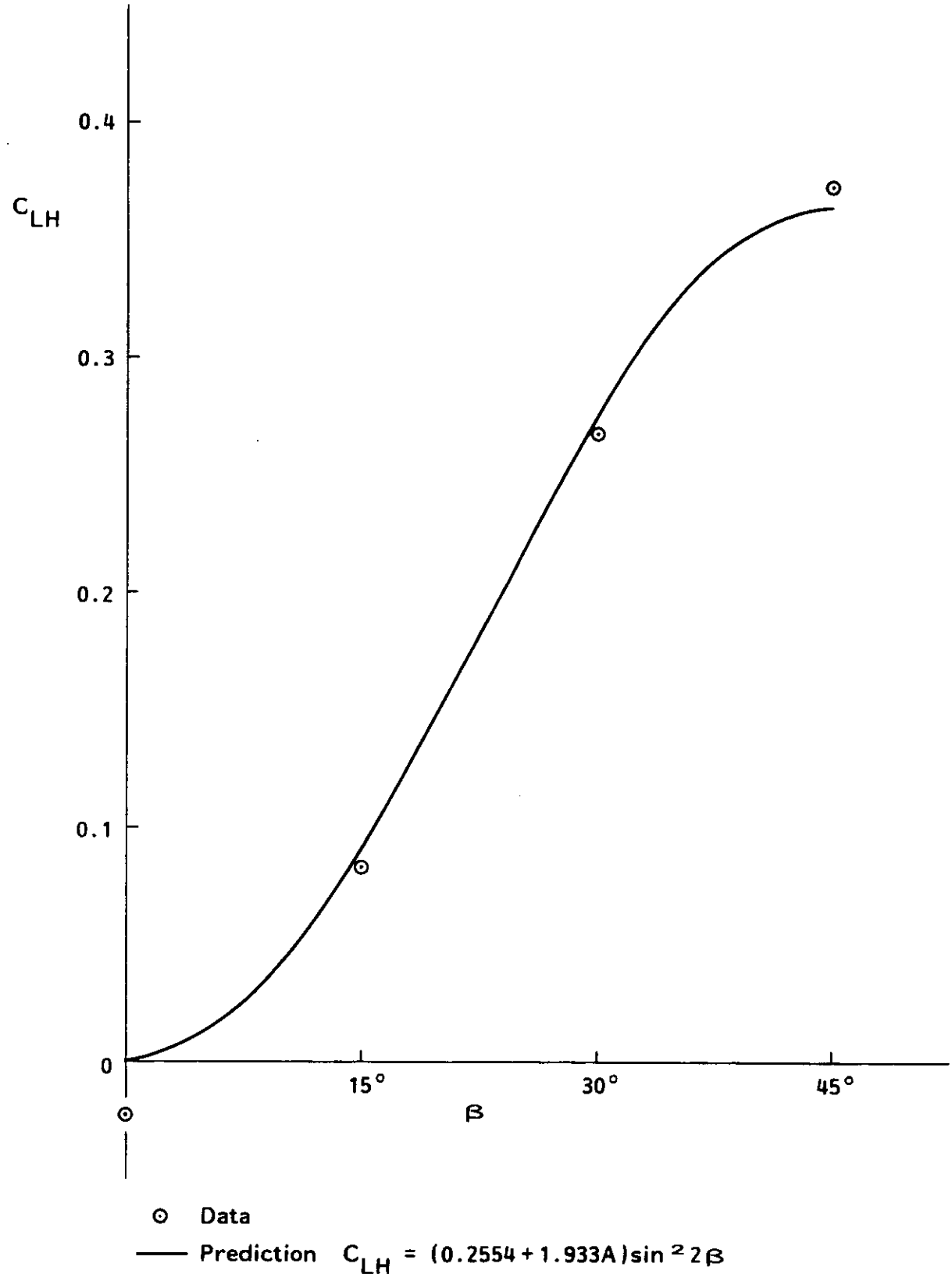

FIG. 2 HULL LIFT COEFFICIENT VERSUS APPARENT WIND ANGLE. (LOAD DRAFT)

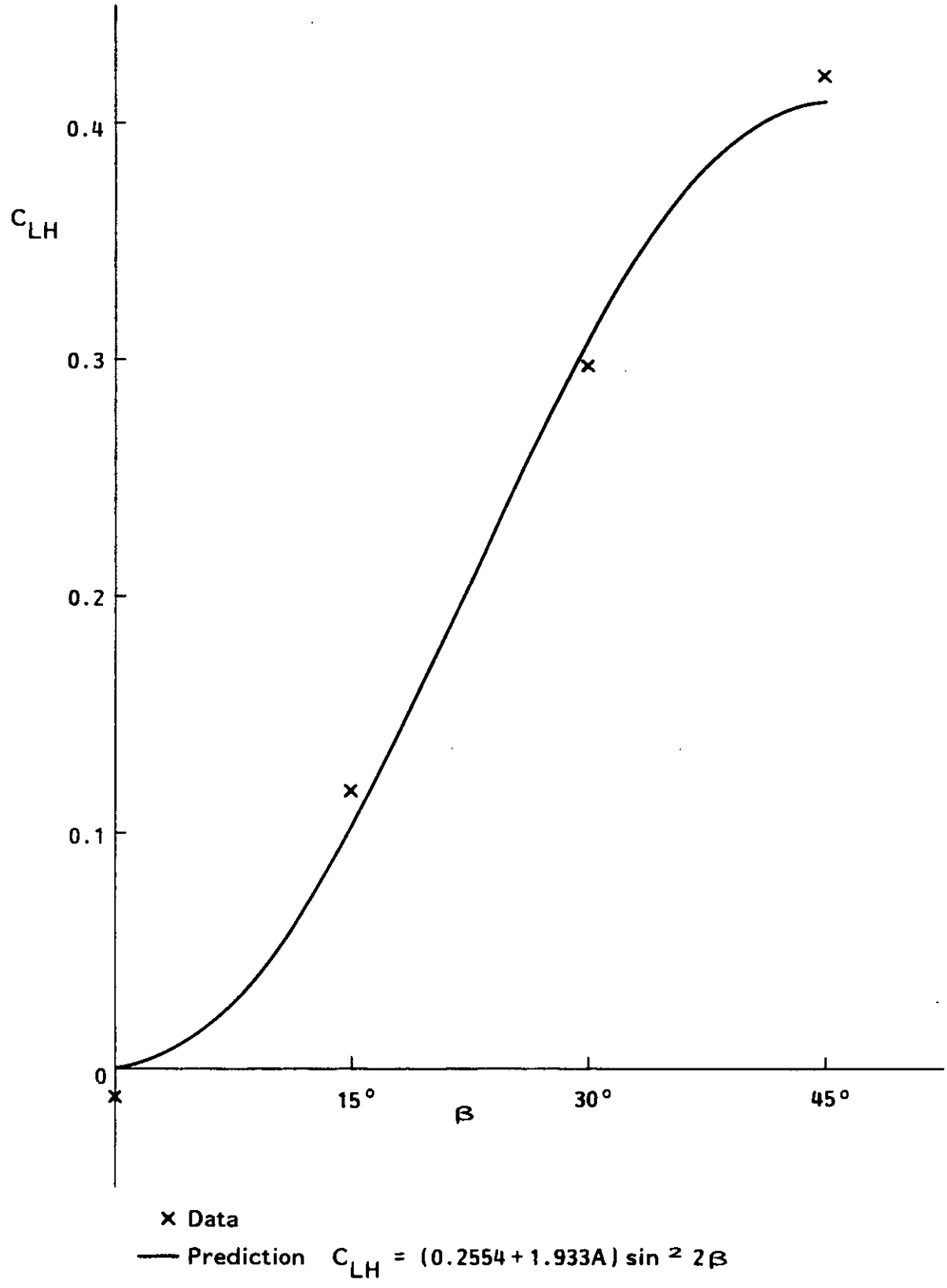

FIG. 3 HULL LIFT COEFFICIENT VERSUS APPARENT WIND ANGLE. (MEDIUM DRAFT)

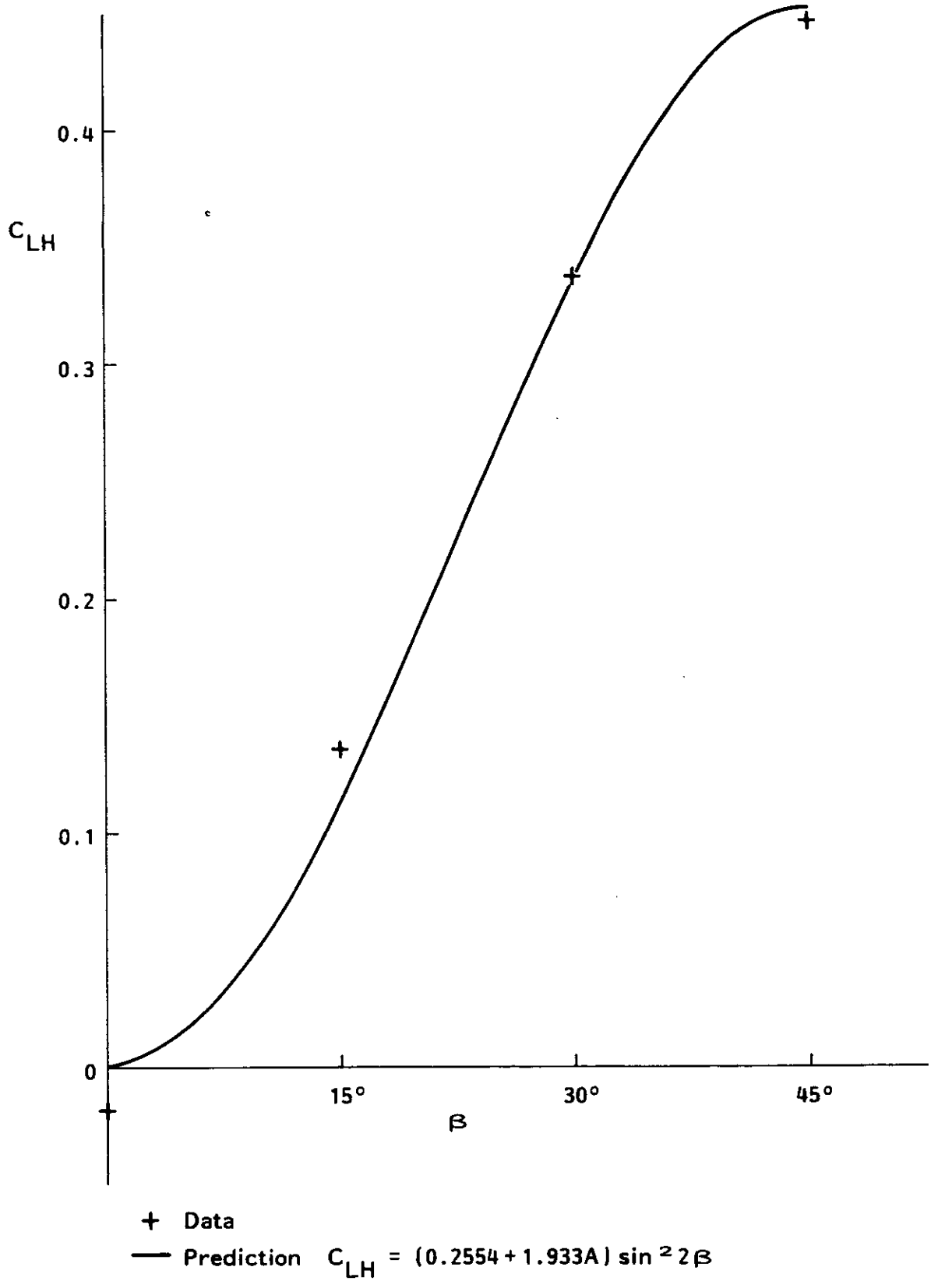

FIG. 4 HULL LIFT COEFFICIENT VERSUS APPARENT WIND ANGLE. (BALLAST DRAFT)

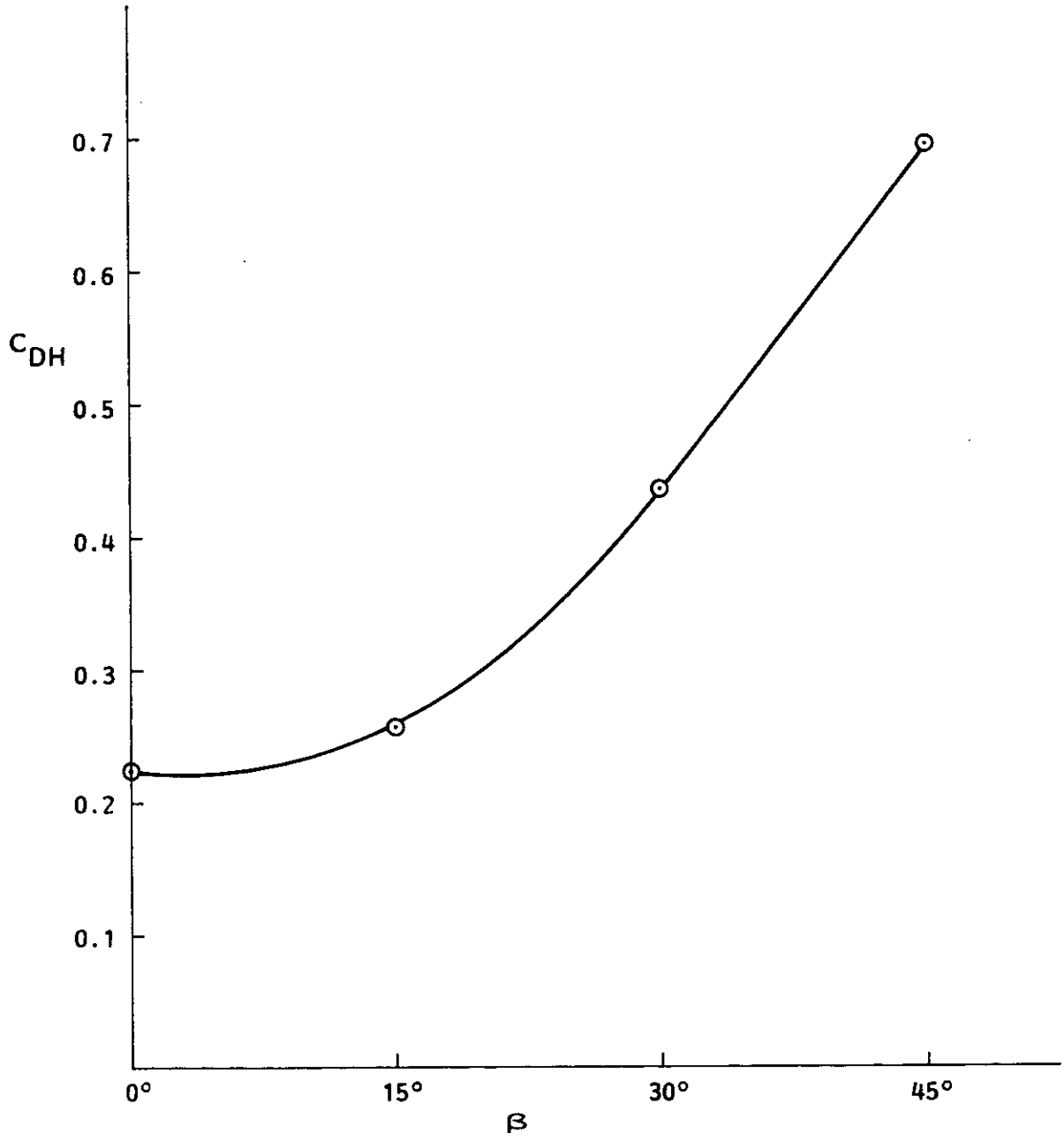

⊙ Data

— Prediction $C_{DH} = \frac{0.030205}{A^{0.6743}} \cos^2\beta + \frac{0.009477}{A^{1.3183}} \sin^2\beta + (0.2554 + 1.933\,A) \tan\beta \sin^2 2\beta$

FIG. 5 HULL DRAG COEFFICIENT VERSUS APPARENT WIND ANGLE. (LOAD DRAFT)

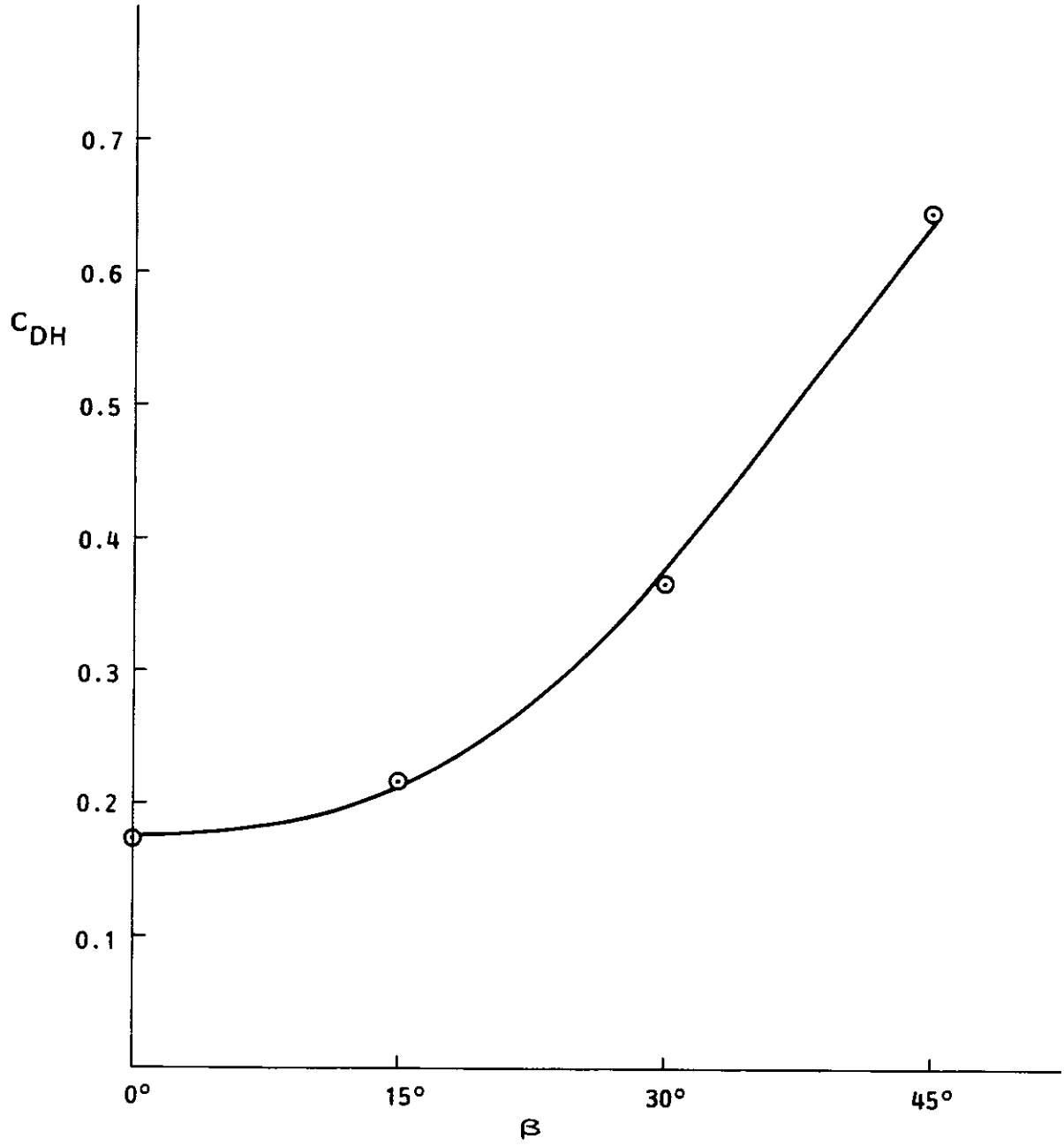

⊙ Data

— Prediction $C_{DH} = \frac{0.03205}{A^{0.6743}} \cdot \cos^2 \beta + \frac{0.009477}{A^{1.3183}} \cdot \sin^2 \beta$

$+ (0.2554 + 1.933\,A) \tan \beta \sin^2 2\beta$

FIG. 6 HULL DRAG COEFFICIENT VERSUS APPARENT WIND ANGLE. (MEDIUM DRAFT)

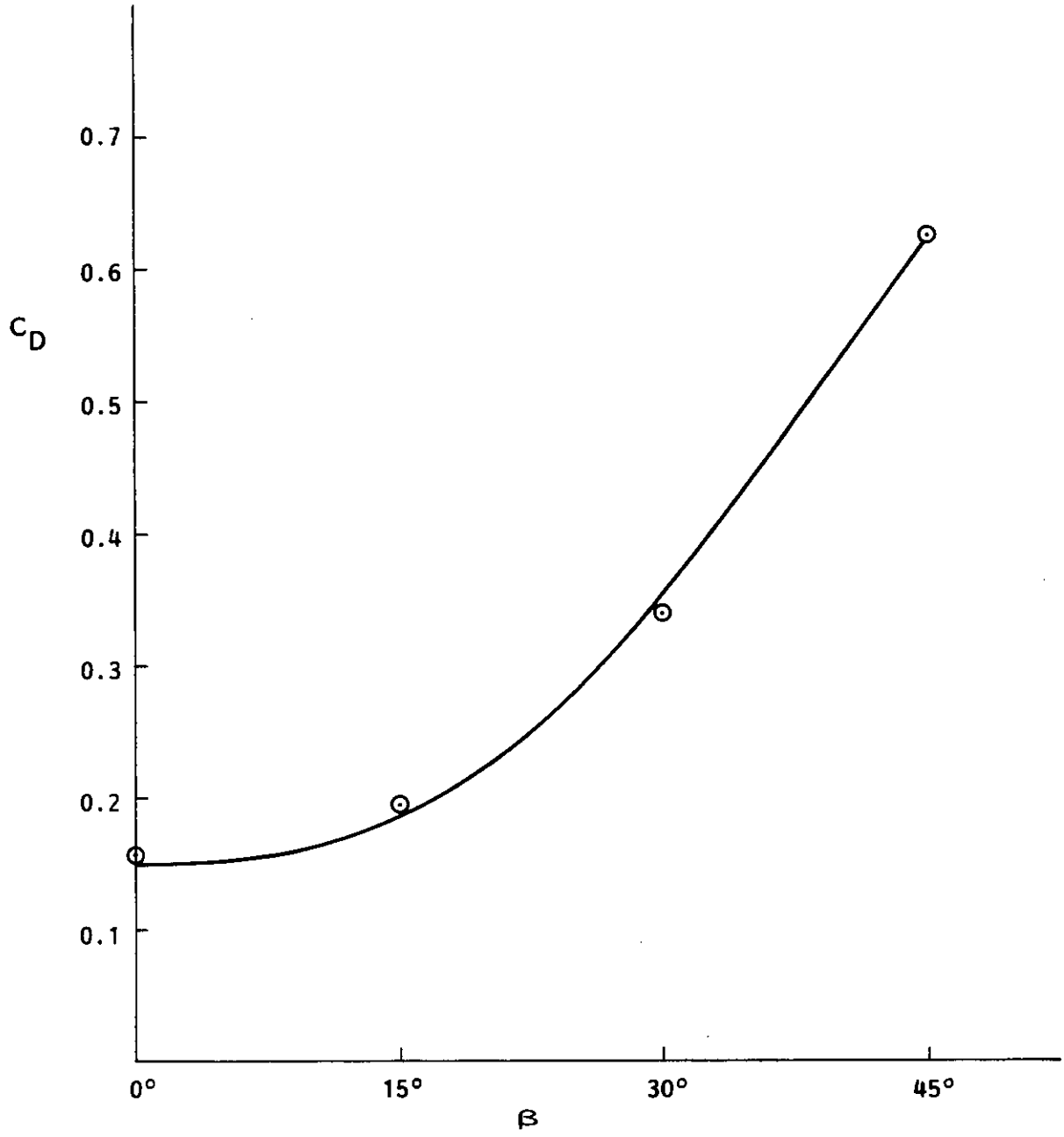

⊙ Data

— Prediction $C_{DH} = \frac{0.03205}{A^{0.6743}} \cos^2 \beta + \frac{0.009477}{A^{1.3183}} \sin^2 \beta + (0.2554 + 1.933\,A) \tan \beta \sin^2 2\beta$

FIG. 7 HULL DRAG COEFFICIENT VERSUS APPARENT WIND ANGLE. (BALLAST DRAFT)

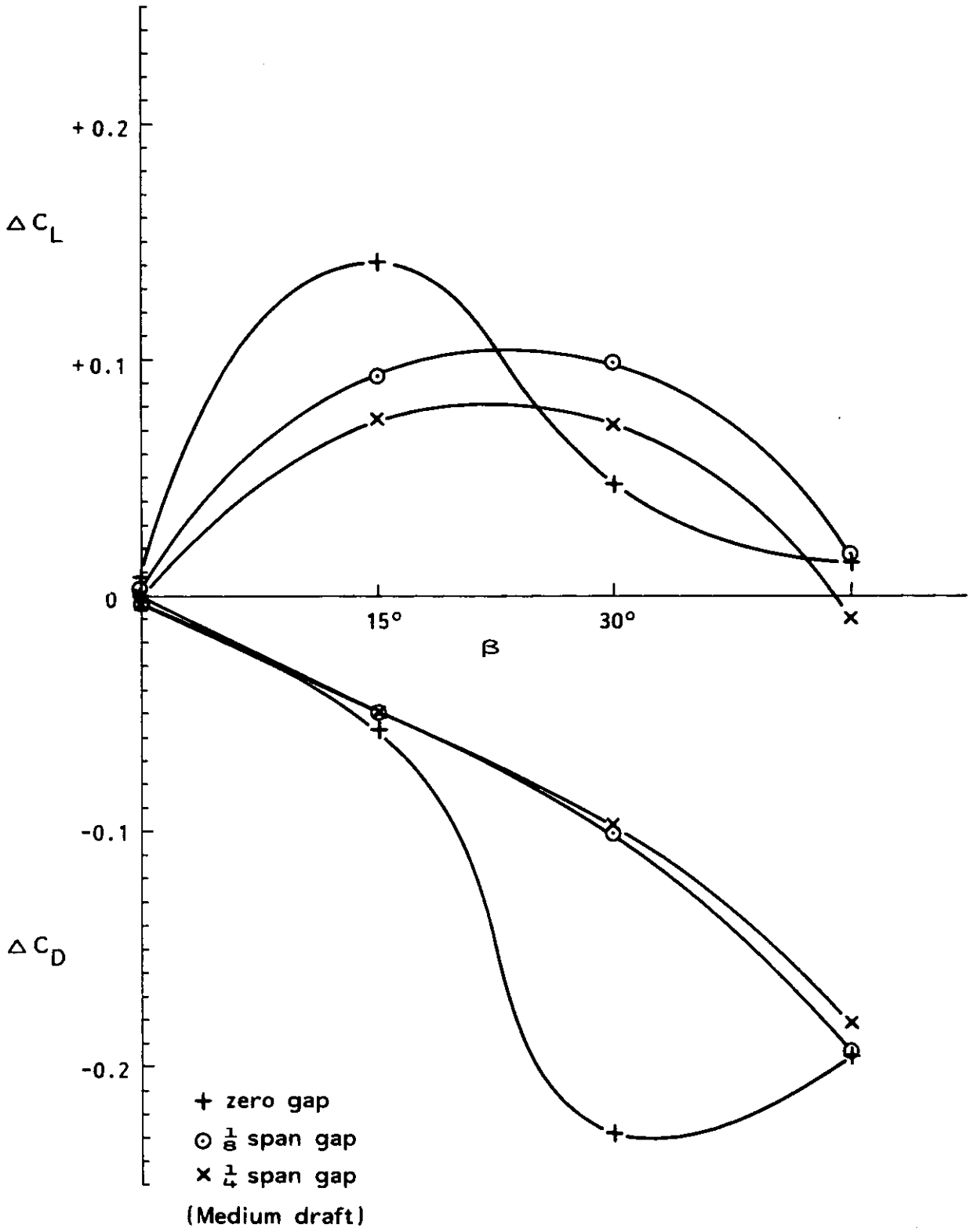

FIG. 8 INTERACTION LIFT AND DRAG COEFFICIENTS - EFFECT OF GAP.

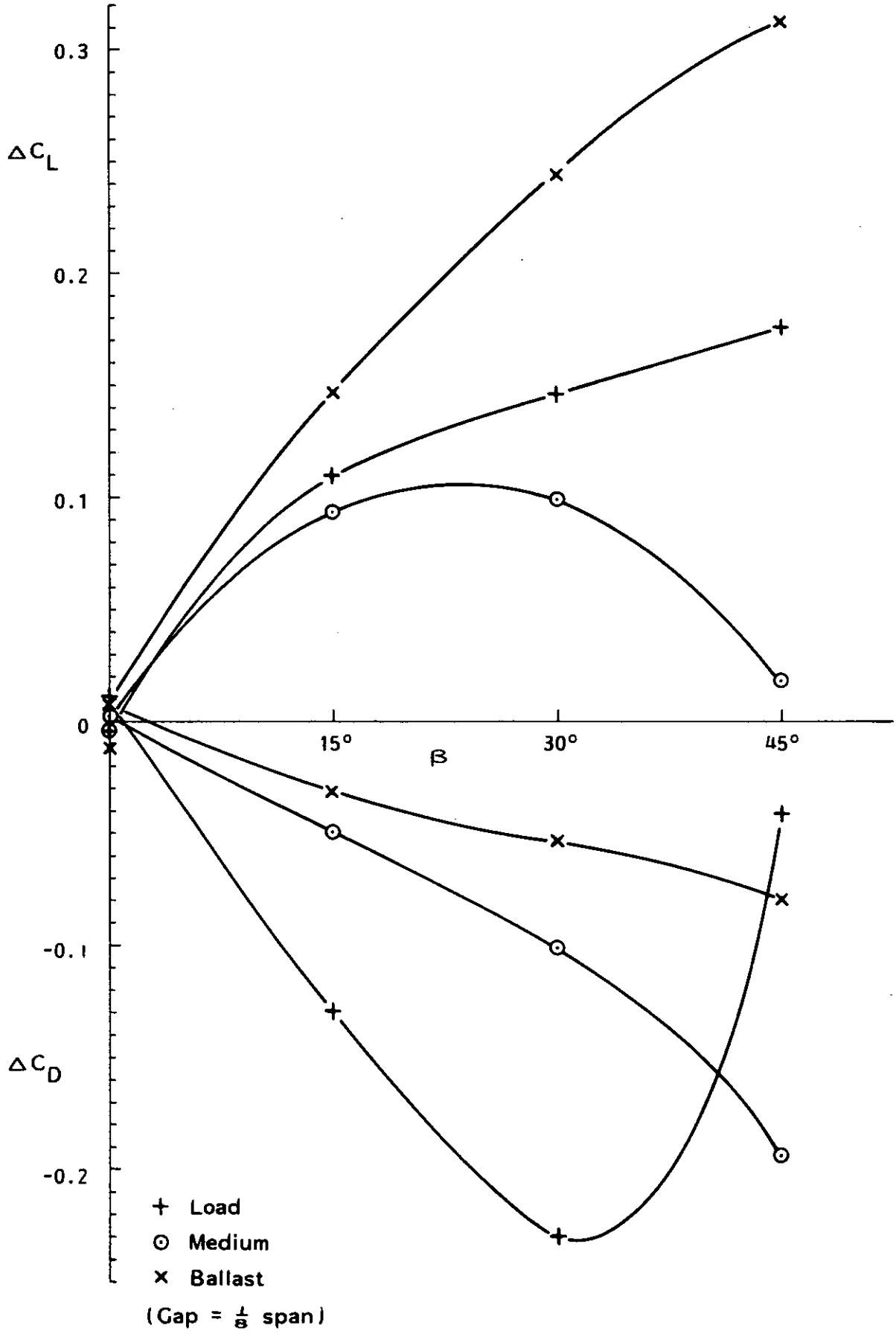

FIG. 9 INTERACTION LIFT AND DRAG COEFFICIENTS - EFFECT OF FREEBOARD (DRAFT).

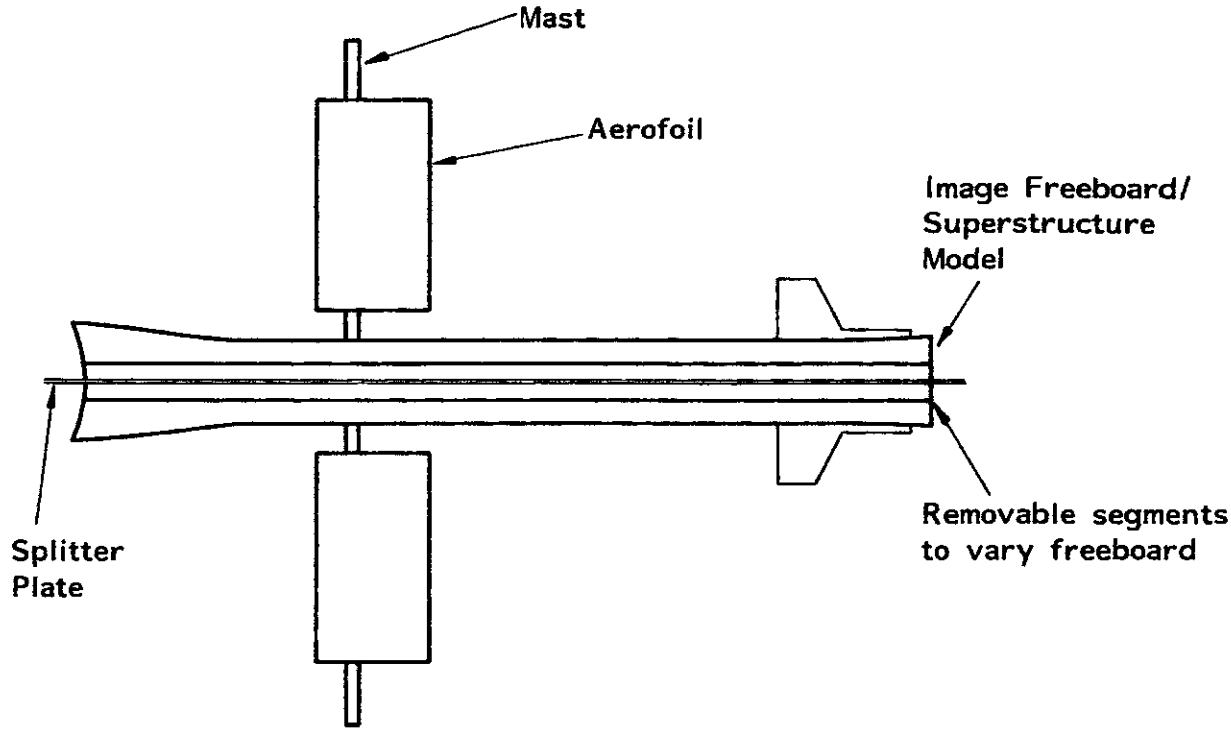

PLAN

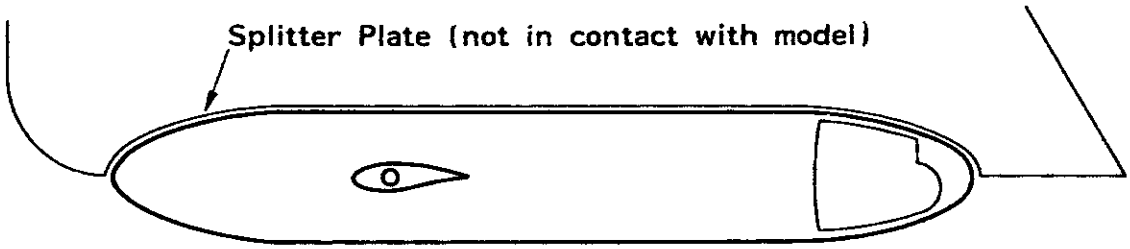

SIDE ELEVATION

$\frac{1}{10}$th scale

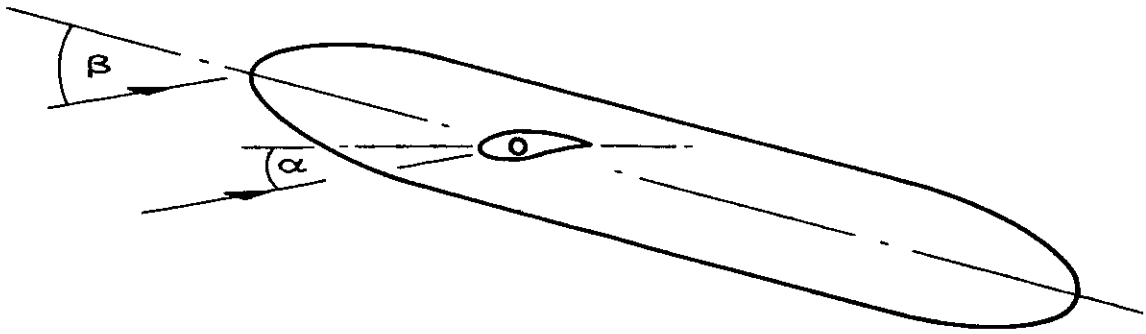

FIG. 1 MODEL DETAILS

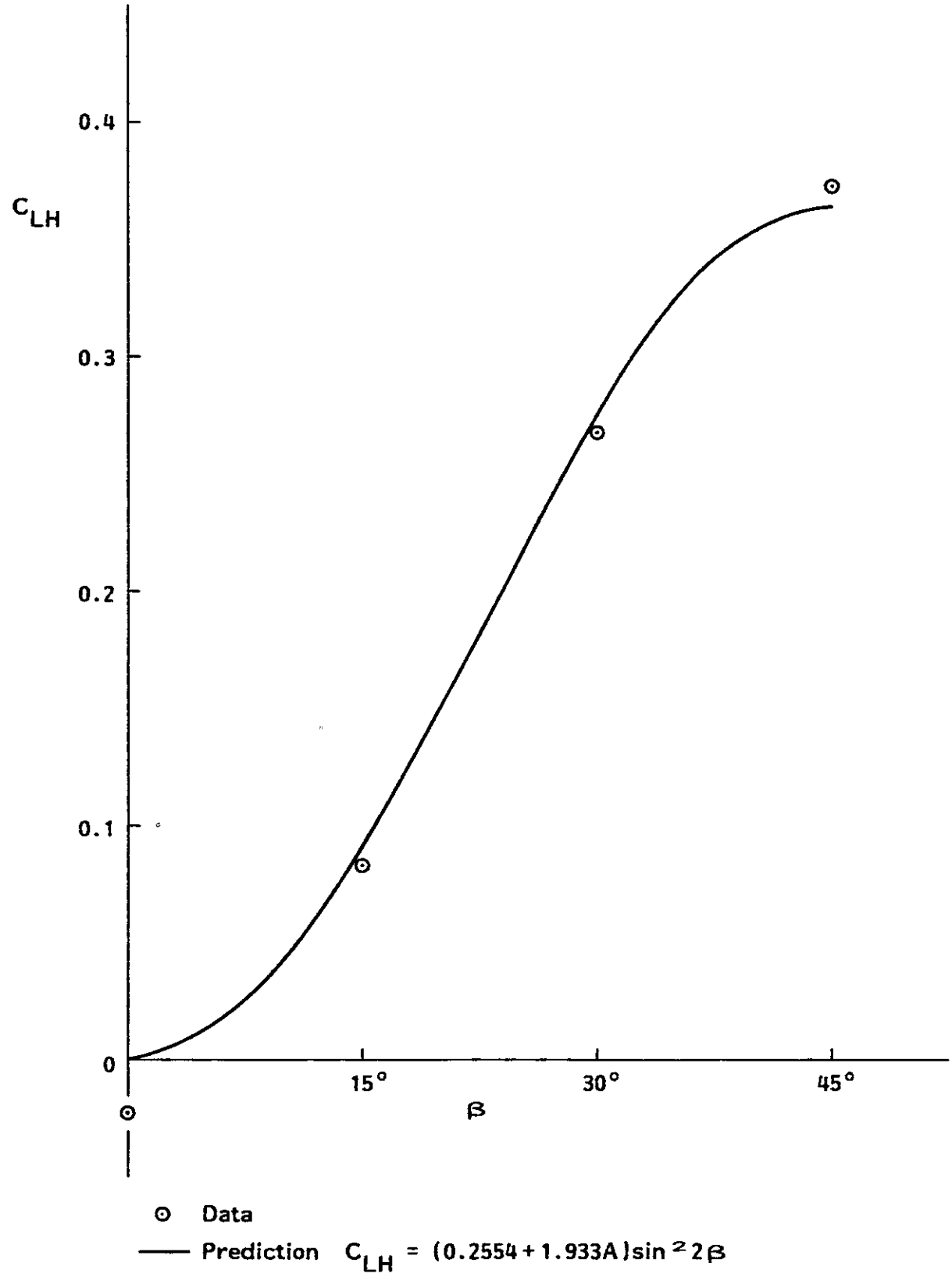

FIG. 2 HULL LIFT COEFFICIENT VERSUS APPARENT WIND ANGLE. (LOAD DRAFT)

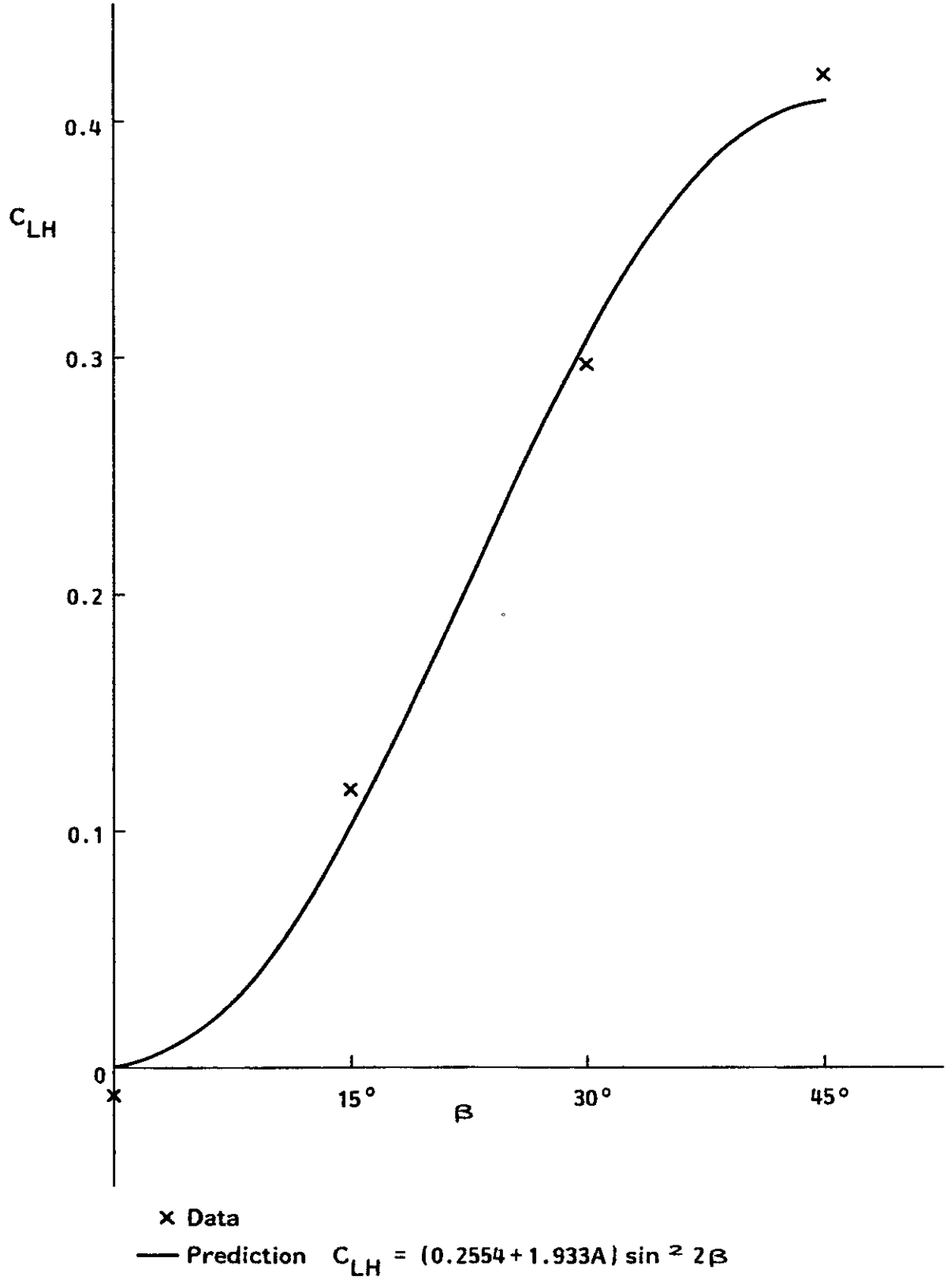

FIG. 3 HULL LIFT COEFFICIENT VERSUS APPARENT WIND ANGLE. (MEDIUM DRAFT)

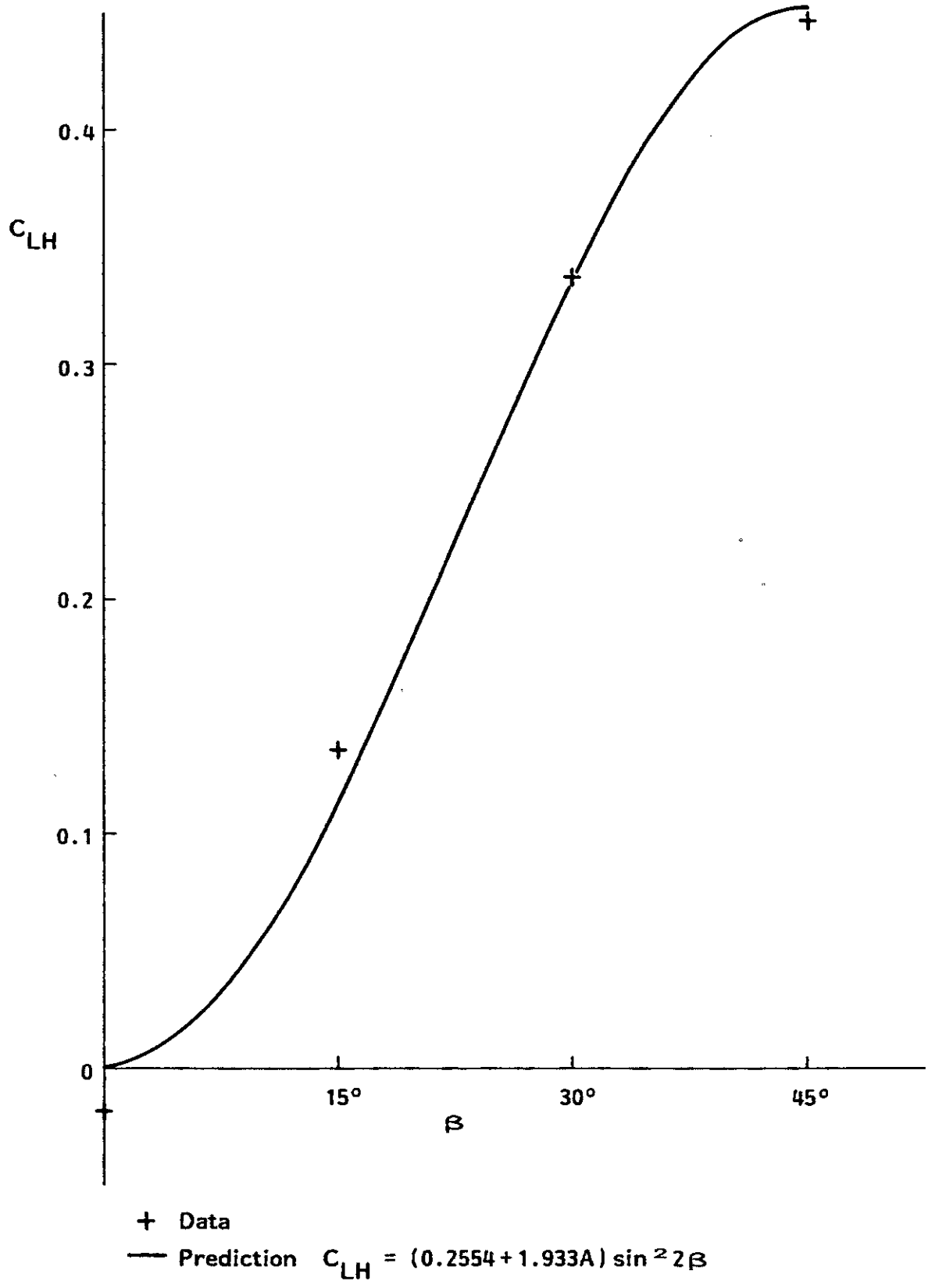

FIG. 4 HULL LIFT COEFFICIENT VERSUS APPARENT WIND ANGLE. (BALLAST DRAFT)

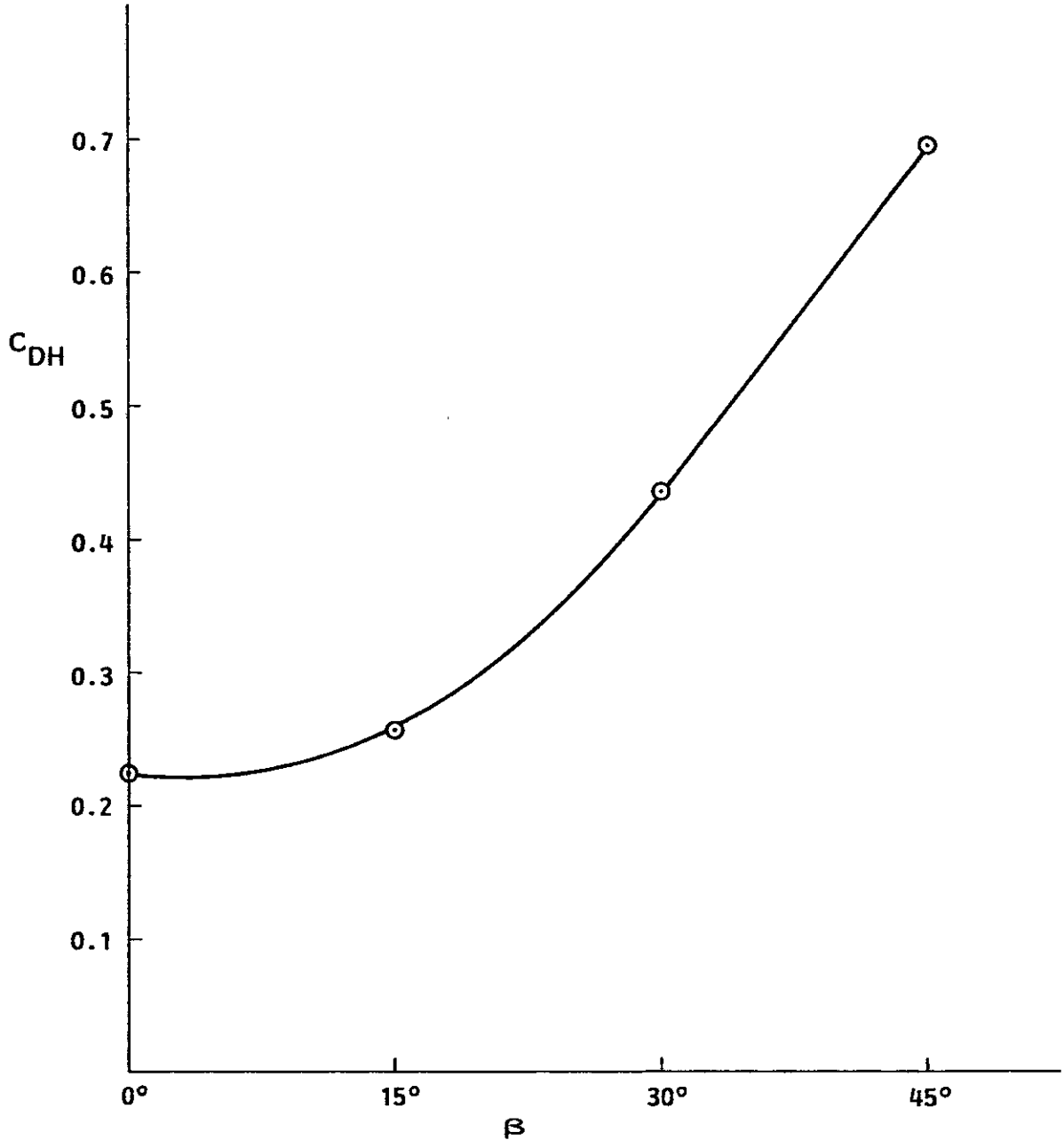

⊙ Data

—— Prediction $C_{DH} = \frac{0.030205}{A^{0.6743}} \cos^2\beta + \frac{0.009477}{A^{1.3183}} \sin^2\beta + (0.2554 + 1.933\,A) \tan\beta \sin^2 2\beta$

FIG. 5 HULL DRAG COEFFICIENT VERSUS APPARENT WIND ANGLE. (LOAD DRAFT)

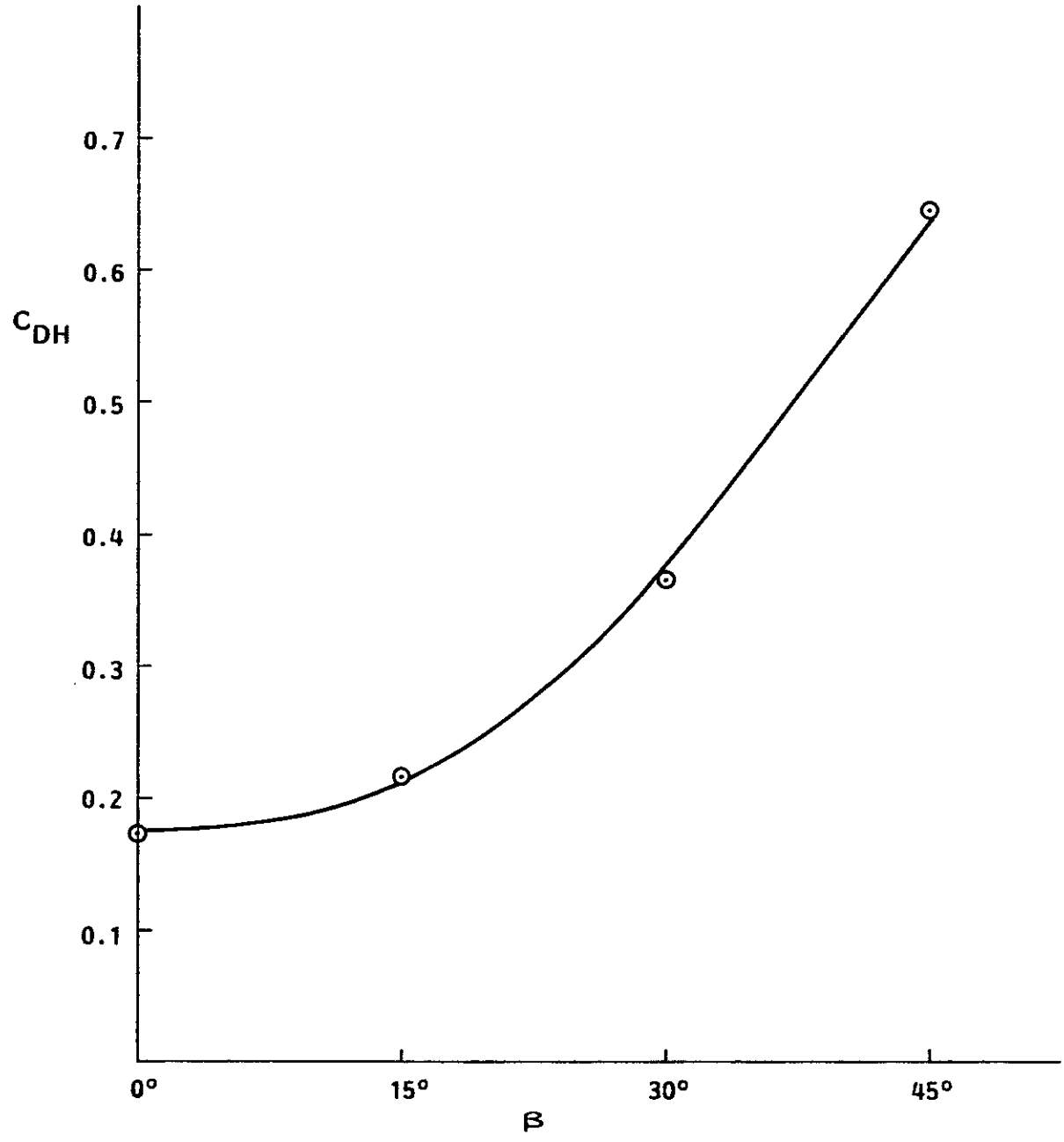

⊙ Data

—— Prediction $C_{DH} = \frac{0.03205}{A^{0.6743}} \cdot \cos^2 \beta + \frac{0.009477}{A^{1.3183}} \cdot \sin^2 \beta$

$+ (0.2554 + 1.933\,A) \tan \beta \sin^2 2\beta$

FIG. 6 HULL DRAG COEFFICIENT VERSUS APPARENT WIND ANGLE. (MEDIUM DRAFT)

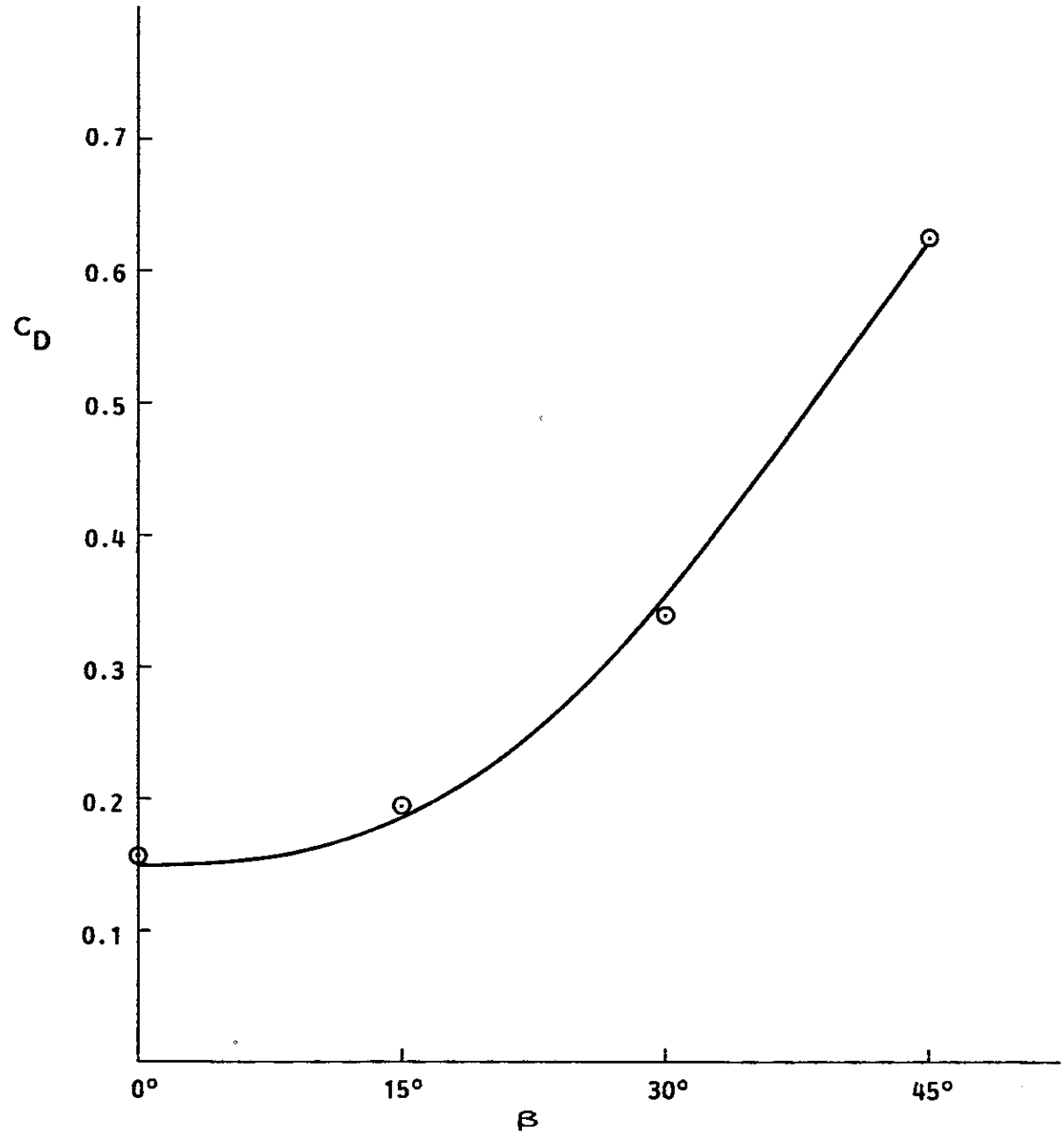

⊙ Data

—— Prediction $C_{DH} = \frac{0.03205}{A^{0.6743}} \cos^2 \beta + \frac{0.009477}{A^{1.3183}} \sin^2 \beta + (0.2554 + 1.933\,A) \tan \beta \sin^2 2\beta$

FIG. 7 HULL DRAG COEFFICIENT VERSUS APPARENT WIND ANGLE. (BALLAST DRAFT)

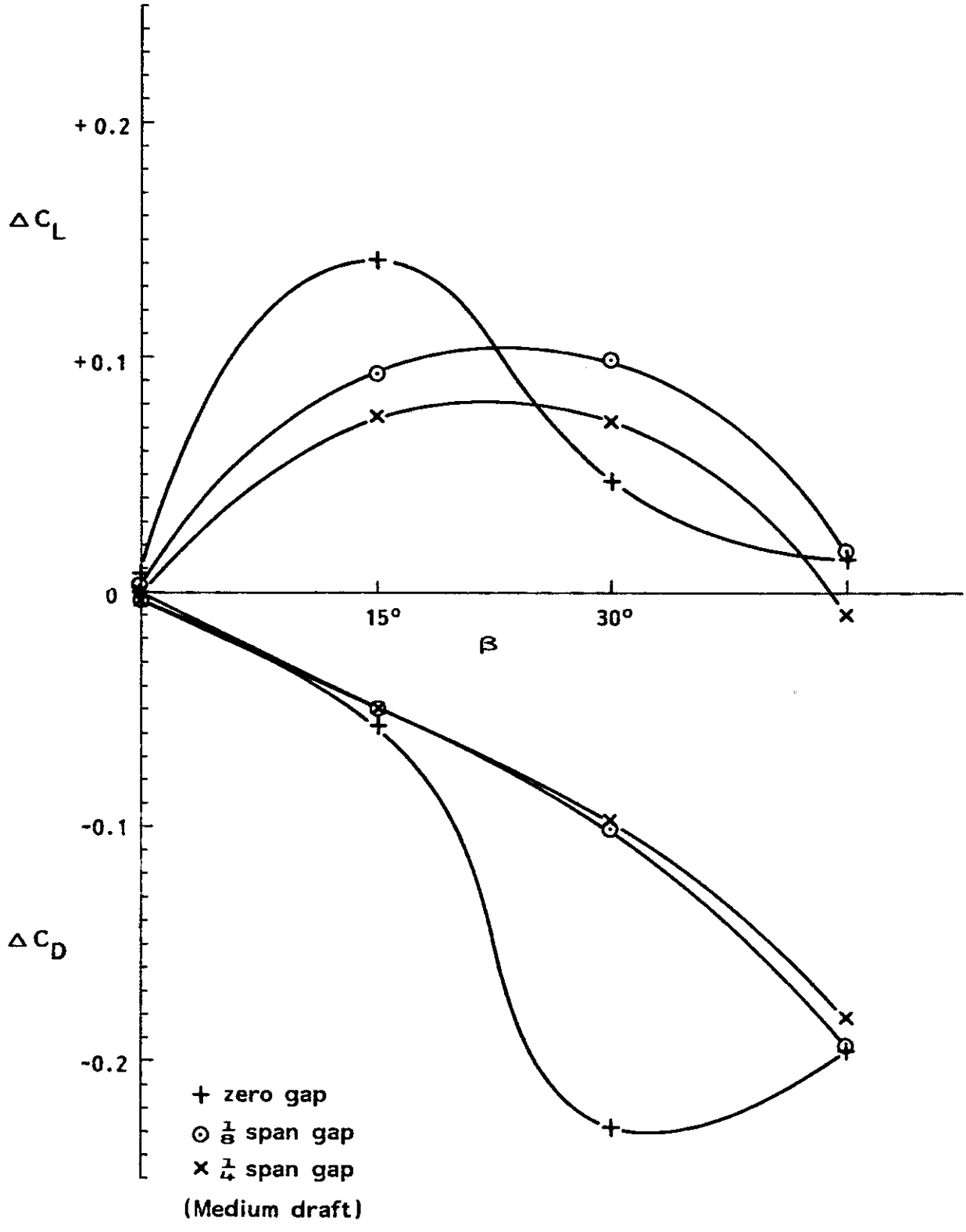

FIG. 8 INTERACTION LIFT AND DRAG COEFFICIENTS - EFFECT OF GAP.

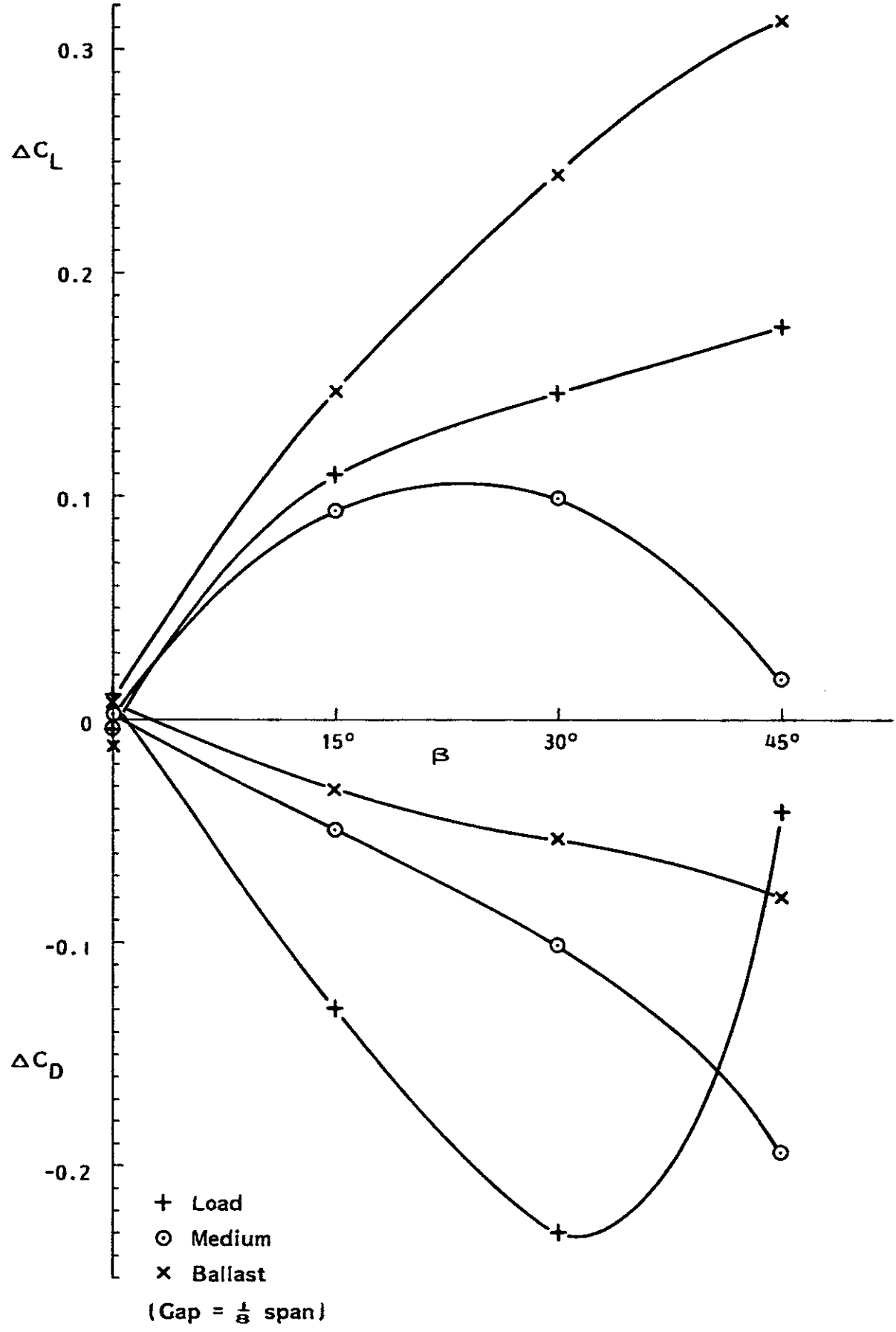

FIG. 9 INTERACTION LIFT AND DRAG COEFFICIENTS - EFFECT OF FREEBOARD (DRAFT).